Original Article

MOLECULAR METABOLISM

Intestinal stem cell-derived enteroids from morbidly obese patients preserve obesity-related phenotypes: Elevated glucose absorption and gluconeogenesis

Nesrin M. Hasan [1,2], Kelli F. Johnson [1], Jianyi Yin [1,3], Nicholas W. Baetz [1], Lea Fayad [1], Vadim Sherman [4], Sarah E. Blutt [5], Mary K. Estes [5], Vivek Kumbhari [1], Nicholas C. Zachos [1,], Olga Kovbasnjuk [1,6,*]**

ABSTRACT

Objective: The mechanisms behind the efficacy of bariatric surgery (BS) for treating obesity and type 2 diabetes, particularly with respect to the influence of the small bowel, remain poorly understood. *In vitro* and animal models are suboptimal with respect to their ability to replicate the human intestinal epithelium under conditions induced by obesity. Human enteroids have the potential to accelerate the development of less invasive anti-obesity therapeutics if they can recapitulate the pathophysiology of obesity. Our aim was to determine whether adult stem cell-derived enteroids preserve obesity-characteristic patient-specific abnormalities in carbohydrate absorption and metabolism.

Methods: We established 24 enteroid lines representing 19 lean, overweight, or morbidly obese patients, including post-BS cases. Dietary glucose absorption and gluconeogenesis in enteroids were measured. The expression of carbohydrate transporters and gluconeogenic enzymes was assessed and a pharmacological approach was used to dissect the specific contribution of each transporter or enzyme to carbohydrate absorption and metabolism, respectively.

Results: Four phenotypes representing the relationship between patients' BMI and intestinal dietary sugar absorption were found, suggesting that human enteroids retain obese patient phenotype heterogeneity. Intestinal glucose absorption and gluconeogenesis were significantly elevated in enteroids from a cohort of obese patients. Elevated glucose absorption was associated with increased expression of SGLT1 and GLUT2, whereas elevated gluconeogenesis was related to increased expression of GLUT5, PEPCK1, and G6Pase.

Conclusions: Obesity phenotypes preserved in human enteroids provide a mechanistic link to aberrant dietary carbohydrate absorption and metabolism. Enteroids can be used as a preclinical platform to understand the pathophysiology of obesity, study the heterogeneity of obesity mechanisms, and identify novel therapeutics.

Keywords Human enteroids; Obesity; Bariatric surgery; Glucose absorption; Gluconeogenesis

1. INTRODUCTION

Obesity is a rapidly growing global health problem that is associated with many obesity-related comorbidities including insulin resistance, type 2 diabetes (T2D), cardiovascular diseases, and cancer [1]. The increasing prevalence of obesity is due to a complex mixture of genetic factors and energy imbalance. Dieting and exercise can yield weight loss; however, it is often modest and transient, with limited improvement in glycemic control [2–4].

Bariatric surgery (BS), which influences intestinal sugar transport and metabolism [5–7], is the most effective and sustainable approach to treat obesity and T2D. Serum glucose concentrations decrease prior to significant weight loss immediately following BS [8,9]. Recent studies showed that glucose absorption in the proximal intestine is elevated in

[1]Department of Medicine, Division of Gastroenterology and Hepatology, Johns Hopkins University School of Medicine, 720 Rutland Avenue, Baltimore, MD 21205, USA [2]Department of Surgery, Yale University School of Medicine, New Haven, CT 06520, USA [3]Department of Internal Medicine, University of Texas Southwestern Medical Center, Dallas, TX 75390, USA [4]Department of Surgery, Minimally Invasive Bariatric and General Division, Houston Methodist Hospital, Houston, TX 77030, USA [5]Department of Molecular Virology and Microbiology, Baylor College of Medicine, One Baylor Plaza, Houston, TX 77030, USA [6]Department of Internal Medicine, University of New Mexico School of Medicine, Albuquerque, NM 87131, USA

*Corresponding author. University of New Mexico Health Sciences Center, Department of Internal Medicine, Division of Gastroenterology and Hepatology, 915 Camino de Salud NE, Building IDTC Room 3330, Albuquerque, NM, 87131, USA. E-mail: OKovbasnjuk@salud.unm.edu (O. Kovbasnjuk).

**Corresponding author. E-mail: nzachos1@jhmi.edu (N.C. Zachos).

Abbreviations: BS, bariatric surgery; UD, undifferentiated; DF, differentiated; GA, glucose absorption; BMI, body mass index; T2D, type two diabetes; BBM, brush border membrane; BLM, basolateral membrane

Received August 31, 2020 • Revision received October 28, 2020 • Accepted November 21, 2020 • Available online 25 November 2020

https://doi.org/10.1016/j.molmet.2020.101129

morbid obesity, contributing to hyperglycemia [10]. However, studies designed to characterize and measure altered glucose absorption in the small intestine from obese patients compared to healthy lean subjects are limited.

Glucose is the main energy source of mammalian cells. Glucose transport is mediated through Na^+ -coupled glucose cotransporters (SGLTs) and facilitative glucose transporters (GLUTs). At low luminal concentrations ($\leq$25 mM), glucose is taken up by enterocytes via SGLT1 expressed at the brush border membrane (BBM) [11,12]. GLUT2 is expressed at the basolateral membrane (BLM) and transports glucose and fructose into the blood [13,14]. At higher luminal glucose concentrations ($\geq$50 mM) such as following a meal, GLUT2 traffics to the BBM resulting in the uptake of excess luminal glucose [15]. Fructose, another dietary sugar, enters enterocytes through GLUT5 at the BBM [16]. At high fructose levels, GLUT2 also localizes to the BBM [17] and contributes to fructose uptake. GLUT1 is expressed at the BLM in enterocytes and has been linked to obesity and diabetes [6,18]; however, its role in intestinal epithelial glucose transport is not well understood.

The expression of intestinal sugar transporters (SGLT1, GLUT2, and GLUT5) is significantly increased in animal models of obesity and/or diabetes [19–21]. Importantly, studies in humans indicate heterogeneous expression [22] and cellular distribution of these major sugar transporters in obesity. GLUT2 was significantly upregulated and continuously present at the BBM of enterocytes in a majority ($\sim$72%) of obese individuals in several studies, while it was absent from the BBM in lean subjects and a subset of obese individuals [23,24]. Conversely, in another study, GLUT2 was not localized apically in duodenal biopsies of overweight T2D subjects [20]. Elevated SGLT1 expression in enterocytes from morbidly obese patients positively correlated with elevated blood glucose; however, the expression of SGLT1 was variable across the studied cohort [10].

De novo glucose production (gluconeogenesis) by intestinal epithelia might also contribute to increased serum glucose levels. Gluconeogenesis primarily occurs in the liver, so studies focused on characterizing the role of intestinal gluconeogenesis are limited and its role in obesity is unclear. Under low luminal fructose conditions, the small intestine metabolizes $\sim$90% of dietary fructose, whereas high doses result in fructose overflow to the liver [25]. Other studies showed that intestinal gluconeogenesis is involved in gut–brain axis signaling and regulation of energy homeostasis [26]. Since portal vein glucose measurements in humans do not separate dietary glucose absorption from *de novo* production, our understanding of how intestinal gluconeogenesis contributes to elevated serum glucose levels is incomplete. Overall, these findings are consistent with the concept that increased intestinal glucose absorption and possibly intestinal gluconeogenesis are associated with hyperglycemia in obesity and T2D. Analysis of human samples implies that the expression and localization of the main glucose and/or fructose transporters is heterogeneous in morbid obesity [10,20,22–24]. On this basis, the molecular classification of inter-individual differences may be a key predictor of the outcome of BS or calorie-restricted diets. Therefore, mechanistic and molecular understanding of the changes in intestinal glucose homeostasis in obesity might be important for generating effective novel therapeutic options as non-invasive alternatives to BS.

To understand the mechanisms involved in the response of the human intestinal epithelia to obesity or BS, it is crucial to have relevant *ex vivo* models. We utilized novel intestinal stem cell-derived epithelial enteroid cultures [27–30] to investigate the contribution of intestinal glucose absorption and gluconeogenesis to the systemic glucose load in lean subjects and obese patients, including post-BS cases. This is the first study to address the relationship between BMI and the expression and function of sugar transporters and gluconeogenic enzymes in a primary model of the human intestinal epithelium and provide evidence that the heterogeneity of obesity-related phenotypes is retained in human enteroids.

2. METHODS

2.1. Human enteroid cultures

Proximal small intestinal tissue samples from either lean healthy (BMI $\leq$ 25 kg/m^2), overweight (25 kg/m^2 $<$ BMI $<$ 35 kg/m^2), or obese (BMI $\geq$ 35 kg/m^2) patients were obtained during routine endoscopy procedures or from discarded tissue from patients undergoing bariatric surgery (BMI $\geq$ 35 kg/m^2). The BMI classification was based on the World Health Organization guidelines. Based on current National Institutes of Health guidelines, the requirements for BS are as follows: BMI $\geq$40 kg/m^2 or BMI $\geq$35 kg/m^2 in patients with obesity-related comorbidities. Information about patient characteristics is provided in Supplementary Table 1. A total of 24 enteroid cultures were successfully established from proximal small intestinal tissue (duodenum or jejunum) obtained from 19 donors. In four of these donors, enteroid cultures were established from biopsies obtained from both the duodenum and jejunum. In one of the donors, enteroid cultures were established from biopsies obtained from different segments of the jejunum. The protocols were approved by Baylor College of Medicine's institutional review board (IRB) (H-31793 and H-31910) and Johns Hopkins' IRB (NA_0038329) and the patients' informed consent was obtained. Crypts were isolated from the de-identified tissue samples and enteroid cultures were established as previously described [27,28,30,31]. Briefly, cells were resuspended in Matrigel (Corning) and cultured in a complete medium (CM) with growth factors ($CMGF^+$ medium). The CM media contained Advanced Dulbecco's Modified Eagle Medium/Ham's F-12 (Life Technologies), 100 U of penicillin/streptomycin (Life Technologies), 10 mM of HEPES (Life Technologies), and 0.2 mM of GlutaMAX (Life Technologies). CMFG + medium was CM medium supplemented with 50% v/v of Wnt3A-conditioned medium, 15% v/v of R-spondin-1-conditioned medium, 10% v/v of Noggin-conditioned medium, 50 ng/ml of human epidermal growth factor (EGF) (Life Technologies), 10 nM of gastrin I (Sigma–Aldrich), 500 nM of A-83-01 (Tocris Bioscience), 10 μM of SB202190 (Sigma–Aldrich), 1 × B27 supplement (Life Technologies), 1 mM of *N*-acetylcysteine (Sigma–Aldrich), 10 μM of CHIR99021 (Tocris Bioscience), and 10 μM of Y-27632 (Tocris Bioscience). The CHIR99021 and Y-27632 were removed from the $CMGF^+$ media during subsequent media replacements. Conditioned media was obtained from the following cell lines expressing the growth factors Wnt3A (CRL-2647 cells, American Tissue Culture Collection), R-spondin-1 (kindly provided by Dr. Calvin Kuo, Palo Alto, CA, USA), and Noggin [32]. Enteroids were passaged every 10–14 days for expansion or monolayer cultures.

2.2. Monolayer plating and differentiation

Enteroid monolayers were prepared as previously described [28]. Briefly, enteroid fragments resuspended in CMGF + media were plated on Transwell filters (Corning #3470; 0.4 μm pores, polyester membranes, and 0.33 cm^2 surface area) coated with 10 μg/cm^2 of human collagen IV solution. Confluent monolayers (or 3D cultures) were differentiated for 5–7 days in differentiation media (CMGF + media lacking Wnt3A, R-spondin, and SB202190). Transepithelial electrical resistance (TER) was measured using an EVOM2 voltohmmeter (World Precision Instruments) to monitor confluency and differentiation of the monolayers.

2.3. Glucose transport experiments

Confluent enteroid monolayers were washed with 5 mM of mannose buffer (50 mM of HEPES pH 7.4, 138 mM of NaCl, 4.7 mM of KCl, 1.25 mM of $MgSO_4$, 1.25 mM of $CaCl_2$, and 5 mM of mannose) and incubated at 37 °C in 5% CO_2 for 30 min (100 μl was added apically to the filter and 600 μl was added basolaterally to the well). An aliquot from the basolateral side was obtained (at $t = 0$), the same mannose buffer volume was added, and the apical solution was replaced with 25 mM or 70 mM of glucose buffer solution. In glucose buffers, the mannose was replaced with glucose and the osmolarity was adjusted by decreasing the NaCl concentration to 128 mM or 105.5 mM. The glucose concentration was determined using an Amplex Red glucose assay kit (Thermo Fisher Scientific). Phloridzin (Sigma—Aldrich), phloretin (Sigma—Aldrich), or STF-31 (Calbiochem) were used as inhibitors. Experimental data were normalized to the glucose absorption value of DF monolayers from enteroid culture #9 of the $BMI^{obese}GA^{high}$ group following 2 h of treatment with 25 mM of apical glucose, and was set at 100%, which allowed a comparison between different enteroid cultures across various experiments.

2.4. Gluconeogenesis experiments

Confluent enteroid monolayers were washed with 5 mM of mannose buffer and incubated for 30 min. Apical solution was replaced by 70 mM of fructose buffer (5 mM of mannose was replaced with 70 mM of fructose, and the NaCl concentration decreased to 105.5 mM) or 2 mM of Na pyruvate/20 mM of Na lactate buffer (5 mM of mannose was replaced with 2 mM of Na pyruvate and 20 mM of Na lactate, and the NaCl concentration decreased to 107 mM). Cells were incubated at 37 °C in 5% CO_2 for 3 h and the solutions were collected for glucose measurements. For 16-h gluconeogenesis experiments, the solutions were modified based on the Advanced DMEM/Ham's F-12 media formulation and supplemented with growth factors. The enteroid monolayers were incubated for 30 min in 5 mM of mannose solution (10 mM of HEPES, pH 7.4, 126.6 mM of NaCl, 4.15 mM of KCl, 0.407 mM of $MgSO_4$, 1.05 mM of $CaCl_2$, 29.02 mM of $NaHCO_3$, 0.3 mM of $MgCl_2$, 0.5 mM of Na_2HPO_4, 0.45 mM of NaH_2PO_4, 5 mM of mannose, 1 × B27 supplement, 1 mM of *N*-acetylcysteine, 50 ng/ml of EGF, 10 nM of gastrin I, and 500 nM of A-83-01). Apical solution was replaced by 70 mM of fructose solution (5 mM of mannose was replaced with 70 mM of fructose, and the NaCl concentration decreased to 94.1 mM). Phloretin (Sigma—Aldrich) or N-[4-(methylsulfonyl)-2-nitrophenyl]-1,3-benzodioxol-5-amine (MSNBA) (Enamine) were used as inhibitors.

2.5. Immunofluorescence

Enteroid monolayers were fixed with 4% paraformaldehyde/PBS for 30 min, washed with PBS, permeabilized, and blocked in PBS containing 15% FBS, 2% BSA, and 0.1% saponin for 45 min. The cells were immunostained using the following antibodies: GLUT1 (ab15309, Abcam), SGLT1 (07—1417, Millipore), and occludin (331500, Life Technologies). The cells were washed with PBS and incubated with secondary antibodies (Life Technologies). Filters were mounted on glass slides using FluorSave Reagent (Millipore). Fluorescent confocal imaging was performed using a 510 LSM (Zeiss) and images were analyzed using MetaMorph software (Molecular Devices).

2.6. Immunoblot analysis

Cells from either 3D cultures or monolayers were harvested, resuspended in lysis buffer, and disrupted by sonication. Protein concentrations were determined using a BCA Protein Assay (Thermo Fisher Scientific). Total cell lysate (25 μg) was mixed with Laemmli loading buffer containing SDS/β-mercaptoethanol. Proteins were separated using Tris-Glycine gels (Thermo Fisher Scientific) and wet-transferred to nitrocellulose membranes. The membranes were blocked using 5% milk/Tris-buffered saline with 0.1% Tween (TBST) and incubated with primary antibodies diluted in 3% BSA/TBST: GLUT1 (ab15309, Abcam), PEPCK1 (HPA006507, Sigma—Aldrich), and GAPDH (G8795, Sigma—Aldrich). The membranes were washed with TBST, incubated with infrared (IR) dye-conjugated secondary antibodies, and imaged using an Odyssey IR Imaging Scanner (LI-COR).

SGLT1 blotting was performed using a modified protocol with cell membrane lysates [33]. Enteroids were resuspended in 25 mM of HEPES, pH 7.4, 250 mM of sucrose, and 1 mM of EDTA solution with protease inhibitor tablets (Roche) and disrupted using a syringe with a 25-gauge needle. Total cell membranes were isolated using differential centrifugation and resuspended in 150 mM of mannitol, 2.5 mM of EGTA, and 12 mM of Tris/HCl at pH 7.4. Total cell membrane (50 μg) was mixed with non-reducing Laemmli loading buffer, denatured at 65 °C, and proteins were separated by 4—12% NuPage gels (Thermo Fisher Scientific) using MOPS buffer. The proteins were wet-transferred to Immobilon PVDF membranes (Millipore) and the membranes were blocked in blotting buffer (5% non-fat dry milk, 0.15 M of NaCl, 1% Triton X-100, and 20 mM of Tris·HCl at pH 7.4). Na/K-ATPase α1-subunit (05369, Millipore) and SGLT1 antibody (provided by Dr. Hermann Koepsell, University of Würzburg, Würzburg, Germany) were diluted in blotting buffer and the membranes were incubated. Washing was performed using blotting buffer, and IR dye-conjugated secondary antibodies were added. The membranes were washed with blotting buffer, followed by a wash using 20 mM of Tris·HCl buffer at pH 7.4 and imaged.

2.7. Real-time polymerase chain reaction

Total RNA was extracted using a PureLink RNA Mini Kit (Ambion) and complementary DNA (cDNA) was synthesized using SuperScript VILO MasterMix (Invitrogen). Quantitative PCR was performed on a QuantStudio 12K Flex Real-Time PCR System (Applied Biosystems). Primer sequences were as follows: GLUT2-fwd (TCTCTGCTACTCTTTTTCTGTCCA), GLUT2-rev (TCATATCCTCTGAGTCTTTTCAAGC), GLUT5-fwd (TCTCCTTGCAAACGTAGATGG), GLUT5-rev (GAAGAAGGGCAGCAGAAGG), glucose-6-phosphatase-fwd (AAGCCGACCTACAGATTTCG), glucose-6-phosphatase-rev (CGTGACAGACAGACATTCAGC), 18S-fwd (GCAATTATTCCCCATGAACG), and 18S-rev (GGGACTTAATCAACGCAAGC).

2.8. Lucifer yellow paracellular permeability

Differentiated confluent enteroid monolayers were washed with 5 mM of mannose buffer and incubated for 30 min. The apical solution was replaced by 5 mM of mannose buffer containing 200 μM of lucifer yellow (MW = 442.3 g/mol). Cells were incubated at 37 °C in 5% CO_2 for 2 h and basolateral solutions were collected for fluorescence measurements.

2.9. Statistical analyses

Statistical analyses were performed using Prism (GraphPad). Student's unpaired t-test was used to analyze for statistical differences with $p < 0.05$ considered statistically significant.

3. RESULTS

3.1. Analysis of the relationship between the subjects' BMI and glucose absorption in enteroid cultures demonstrated three phenotypes

Duodenal and/or jejunal small intestinal tissue samples were collected from 19 donors including naturally lean subjects, overweight patients,

morbidly obese patients, and post-BS lean patients (Supplementary Table 1 and Supplementary Fig. 1). Enteroid cultures were generated from 24 tissue samples (from the 19 donors) to study the mechanistic differences in dietary sugar absorption and metabolism as a function of BMI. The absorption (defined as transcellular transport of nutrients from the lumen across the intestinal epithelium to the blood) of dietary sugars mainly occurs in the proximal small intestine (duodenum and jejunum). Enterocytes of small intestinal villi, but not immature enterocytes in the crypts, are mainly responsible for carbohydrate absorption [34]. To measure the absorption of luminal sugar, confluent enteroid monolayers were grown on Transwell filters, which allowed access to both apical and basolateral surfaces [28,29] and modeled as crypt-like or villus-like epithelia using undifferentiated (UD) or differentiated (DF) enteroid monolayers, respectively [27,28,31].

DF monolayers derived from the 24 tissue samples were exposed to 25 mM of glucose apically and changes in the glucose concentration were measured in basolateral media as an indicator of glucose absorption. Four phenotypes representing the correlation between BMI and glucose absorption (GA) were found (Figure 1A): $BMI^{lean}GA^{low}$, $BMI^{obese}GA^{high}$, $BMI^{obese}GA^{low}$, and $BMI^{overweight}GA^{high}$. Enteroids from obese patients had two glucose-absorption phenotypes (GA^{low} or GA^{high}). Enteroids from overweight patients exhibited similar glucose absorption to the $BMI^{obese}GA^{high}$ group. These data provide evidence for the heterogeneity of glucose absorption reported in morbidly obese patients [10,20,22–24] and suggest that elevated intestinal glucose absorption in a subset of obese patients may potentially contribute to hyperglycemia.

We next confirmed that the difference in glucose absorption between the $BMI^{lean}GA^{low}$ and $BMI^{obese}GA^{high}$ groups was due to transcellular transport. The epithelial cell barrier integrity of the DF monolayers was assessed through transepithelial electrical resistance (TER). The TER among the $BMI^{lean}GA^{low}$, $BMI^{obese}GA^{high}$, $BMI^{obese}GA^{low}$, and $BMI^{overweight}GA^{high}$ groups was similar, suggesting that the difference in glucose absorption was not due to transepithelial leakage of macromolecules (Supplementary Fig. 2A). To test the permeability of tight junctions, we exposed DF monolayers apically with lucifer yellow, a low molecular weight paracellular flux tracer. The fluorescence levels of lucifer yellow in the basolateral media were similar (Supplementary Fig. 2B), indicating that differences in glucose absorption between the $BMI^{lean}GA^{low}$ and $BMI^{obese}GA^{high}$ groups were based on transcellular transport and not due to glucose leak across tight junctions. Glucose absorption and epithelial permeability measurements retained similar trends over the duration of the experiments (~15 passages) in the enteroid lines used in this study.

We next compared the physiological and molecular mechanisms of sugar absorption and metabolism between the BMI^{lean} and BMI^{obese} phenotypes in enteroid monolayers. To determine whether successful BS might reduce glucose absorption to levels in naturally lean conditions, enteroids from the $BMI^{lean}GA^{low}$ phenotype were divided into two groups: 1) BS naïve or 2) sustainably lean post-BS and analyzed separately.

3.2. Changes in luminal glucose concentrations differentially affected glucose absorption in enteroids with $BMI^{lean}GA^{low}$ phenotypes compared to $BMI^{obese}GA^{high}$ phenotypes

We measured glucose absorption in DF and UD jejunal enteroids exposed apically to 25 mM of glucose (to mimic a low-carbohydrate meal). Glucose absorption was higher in the DF monolayers than the phenotype-matched UD monolayers in all of the groups (Figure 1B). The glucose absorption of the $BMI^{obese}GA^{low}$ phenotype was similar to the $BMI^{lean}GA^{low}$ phenotype. Glucose absorption in enteroids derived from successful post-BS surgery was similar to that from naturally lean subjects (Figure 1B). The absorption in the DF monolayers from the $BMI^{obese}GA^{high}$ group was significantly higher than the DF monolayers with low glucose absorption. Glucose absorption values of the DF monolayers after 2 h of treatment with 25 mM of apical glucose from a representative experiment were 40.1 ± 5.3 μM ($BMI^{lean}GA^{low}$), 30.3 ± 5.5 μM ($BMI^{lean}GA^{low}$ (post-BS)), 37.1 ± 2.2 μM ($BMI^{obese}GA^{low}$), and 260.4 ± 31.5 μM ($BMI^{obese}GA^{high}$). Strikingly, UD

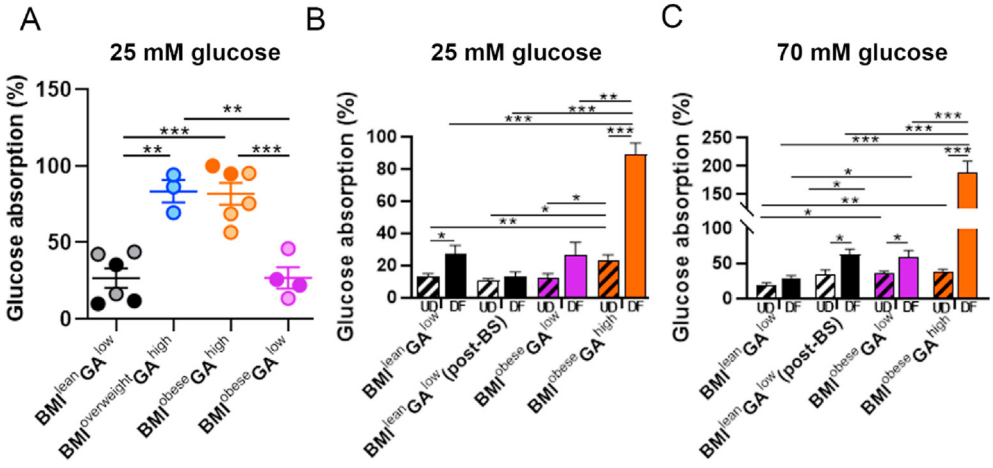

Figure 1: Relationship between subjects' BMI and transepithelial (apical to basolateral) glucose absorption in enteroid monolayers. Glucose absorption in DF monolayers treated apically with 25 mM of glucose for 120 min (24 enteroid cultures representing 19 subjects). Each data point represents the mean of glucose absorption per donor obtained from at least three independent experiments. The mean in each phenotype group represents the mean ± SEM of glucose absorption from different donor cultures belonging to the same BMI-GA phenotype. BS naïve enteroid cultures in each group are represented as dark color-filled circles, whereas the post-BS enteroid cultures are represented by the light color-filled circles. (B and C) Glucose absorption in UD and DF monolayers from four representative jejunal enteroid cultures treated apically with 25 mM of glucose (B) or 70 mM of glucose (C) for 120 min. (A–C) Experimental data were normalized to the glucose absorption value at 25 mM of luminal glucose in the DF monolayers from enteroid culture #9 of the $BMI^{obese}GA^{high}$ group and was set as 100%, which allowed the comparison between different enteroid cultures across various experiments. Each independent experiment included at least three technical replicates per enteroid culture. Data from up to six independent experiments are presented as mean ± SEM; *$p \leq 0.05$, **$p \leq 0.01$, and ***$p \leq 0.001$ using Student's two-tailed t-test. The BMI classification is based on the World Health Organization guidelines. GA classification is based on the median value (50.2) of GA at 25 mM of glucose treatment in the studied enteroids. GA, glucose absorption; BMI, body mass index; UD, undifferentiated; DF, differentiated.

monolayers from the BMI^{obese}GA^{high} phenotype absorbed a significantly higher amount of glucose (~3-fold) than the UD monolayers from both lean groups, indicating that crypt-based epithelial cells might also contribute to the elevated sugar absorption in obesity. Kinetic analysis showed that the differences in the basolateral glucose concentration between the BMI^{lean}GA^{low} and BMI^{obese}GA^{high} groups were already significant at 30 min after exposure to apical glucose in both the DF and UD monolayers (Supplementary Fig. 3A and B). We concluded that following treatment with 25 mM of glucose, the intestinal epithelium derived from a subpopulation of morbidly obese patients absorbs significantly more glucose than the epithelium derived from lean subjects. Additionally, the BMI^{obese}GA^{low} phenotype had glucose absorption similar to the BMI^{lean} group, suggesting that obesity is a complex metabolic disease and pathways other than intestinal glucose absorption might be involved.

To mimic the effects of a high-carbohydrate meal, 70 mM of glucose was added apically to the monolayers. The absorption in the DF monolayers from the BMI^{obese}GA^{high} group was significantly higher than the DF monolayers from all three groups with low glucose absorption. The difference was highest (~6.0-fold) in comparison to the BS naïve BMI^{lean}GA^{low} group (Figure 1B). The time course further confirmed significant differences in basolateral glucose concentrations between the BS naïve BMI^{lean}GA^{low} and BMI^{obese}GA^{high} groups at all of the studied time points (Supplementary Fig. 3C and D). Contrary to 25 mM of apical glucose, 70 mM of apical glucose treatment of the DF monolayers representing the BMI^{obese}GA^{low} phenotype showed significantly higher glucose absorption (~2-fold) than the BS naïve BMI^{lean}GA^{low} enteroids (Figure 1C). Monolayers from the BMI^{lean}GA^{low} (post-BS) group exposed to high luminal glucose behaved similar to the BMI^{obese}GA^{low} group. Glucose absorption values of the DF monolayers after 2 h of treatment with 70 mM of apical glucose from a representative experiment were 99.2 $\pm$ 5.8 μM (BMI^{lean}GA^{low}), 165.3 $\pm$ 17.5 μM (BMI^{lean}GA^{low} (post-BS)), 169.1 $\pm$ 13.5 μM (BMI^{obese}GA^{low}), and 440 $\pm$ 20.2 μM (BMI^{obese}GA^{high}). These data indicated that post-BS epithelium in lean subjects differed from the epithelium from the BS naïve lean subjects in which intestinal epithelial glucose absorption remained low regardless of the luminal glucose concentrations.

We concluded that the glucose absorption in the enteroids from the BMI^{obese}GA^{high} phenotype correlated with the increase in the luminal dietary glucose concentration and appeared to not reach saturation. Importantly, at high apical glucose concentrations, the glucose absorption by the UD monolayers from the BMI^{obese} GA^{high} group was similar to the glucose absorption by the DF monolayers from the BMI^{lean}GA^{low} group, further suggesting the contribution of crypt-like epithelium to high glucose in obesity.

A high rate of concordance in the transcriptome of intestinal organoids and intestinal primary tissue has been shown [35,36], indicating that intestinal organoids preserve donor phenotypes. Based on these published observations, our data suggested that measured differences in epithelial glucose handling between enteroid cultures representing lean or obese phenotypes are likely to reflect the intrinsic trait of the donor intestinal epithelium. Overall, our results indicated that enteroids are a relevant patient-specific model to study obesity-imposed intestinal epithelial pathologies.

3.3. Expression levels of transporters involved in dietary carbohydrate absorption were significantly altered in enteroids from the BMI^{obese}GA^{high} phenotypes compared to the BMI^{lean}GA^{low} phenotypes

To understand the mechanisms responsible for the increased glucose absorption in obesity, we focused on the expression and localization of major carbohydrate transporters SGLT1, GLUT2, and GLUT5 in enteroids from the BMI^{obese}GA^{high} and BMI^{lean}GA^{low} phenotypes using immunoblotting, immunofluorescence, or qRT-PCR (in the absence of reliable antibodies).

SGLT1 expression was significantly upregulated in all of the groups upon differentiation, consistent with physiological data that villus enterocytes are mainly involved in dietary glucose absorption. Interestingly, the magnitude of SGLT1 upregulation due to differentiation was significantly higher (~4-fold) in the BMI^{obese}GA^{high} group than the BMI^{lean}GA^{low} phenotype (~2.5-fold) (Figure 2A,B). SGLT1 colocalized with F-actin and wheat germ agglutinin at the apical surface of human monolayers (Supplementary Fig. 4A and B). The fluorescence intensity of SGLT1 was higher in monolayers from the BMI^{obese}GA^{high} group than the BMI^{lean}GA^{low} group (Figure 2C). These data support our glucose transport findings, demonstrating a link between increased apical expression of SGLT1 and increased glucose absorption in BMI^{obese}GA^{high} enteroids.

Similar to SGLT1, *GLUT2* mRNA expression was similar in the UD monolayers and significantly increased in the DF monolayers in all three groups, since dietary glucose absorption was mostly accomplished by villus enterocytes (Figure 3A). DF monolayers representing the BMI^{obese}GA^{high} phenotype had higher *GLUT2* mRNA expression (~23-fold) than those from the BS naïve BMI^{lean}GA^{low} group. These data together with the functional assessment of the contribution of GLUT2 to glucose absorption using phloretin indicated that GLUT2 significantly contributes to elevated glucose absorption in obesity.

To determine whether fructose absorption was affected, the mRNA levels of *GLUT5* were measured. *GLUT5* mRNA expression was similar in the UD monolayers in the BMI^{lean}GA^{low} and BMI^{lean}GA^{low} (post-BS) cultures but significantly higher (~35-fold) in the UD monolayers of the BMI^{obese}GA^{high} phenotype. *GLUT5* mRNA expression significantly increased upon differentiation, and the BMI^{obese}GA^{high} DF monolayers had significantly higher GLUT5 mRNA expression (~150-fold) than the BS naïve enteroids (Figure 3B). These data, together with the GLUT5 inhibition data, suggested that fructose absorption may also have been higher in the monolayers from the BMI^{obese}GA^{high} phenotype than the lean phenotype.

Taken together, our data indicated that in the BMI^{obese}GA^{high} enteroids, obesity was associated with significant changes in expression of the major carbohydrate transporting proteins SGLT1, GLUT2, and GLUT5. Importantly, human enteroids in long-term cultures preserved these obesity-related differences in the expression of carbohydrate transporters.

3.4. Inhibition of intestinal sugar transporters SGLT1 and GLUT2 significantly decreased glucose absorption in enteroid monolayers from the BMI^{obese}GA^{high} phenotypes

Both the increase in luminal dietary glucose uptake and basolateral secretion by enterocytes may be responsible for the elevated absorption of glucose reaching the bloodstream. We next examined the contribution of glucose transporters SGLT1 and GLUT2 to the overall glucose absorption using pharmacological studies. The DF monolayers (highest glucose absorption as shown in Figure 1) were exposed to either 25 mM (Figure 4A) or 70 mM of glucose (Figure 4B) with phloretin (PT, a GLUT2 inhibitor) or phloridzin (PZ, an SGLT1 inhibitor) [15,37,38]. Either PT (50 μM) or PZ (50 μM) treatments significantly decreased glucose absorption compared to untreated controls. The combination of PT and PZ did not further decrease the basolateral glucose concentration (Figure 4), indicating that both SGLT1 and GLUT2 are involved in the same glucose absorption pathway.

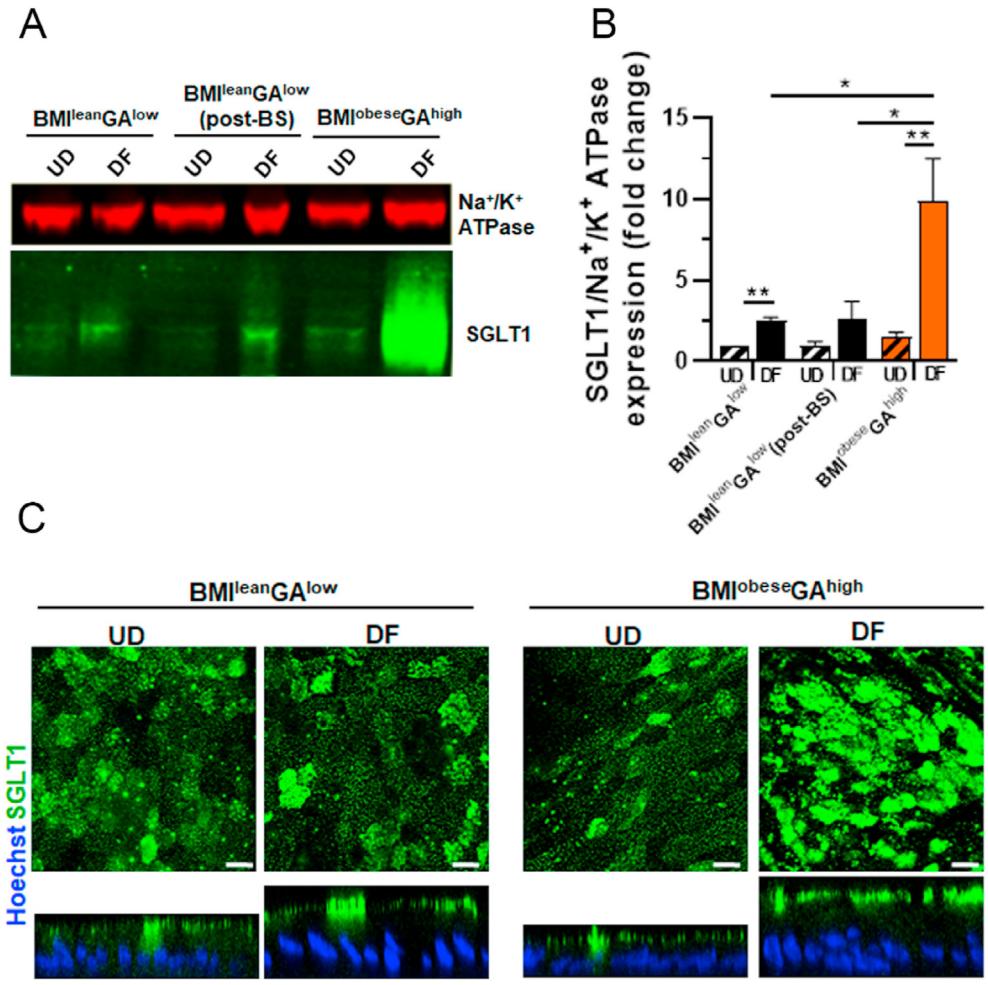

Figure 2: SGLT1 was significantly upregulated in enteroid cultures derived from the BMI^{obese}GA^{high} phenotype compared to the BMI^{lean}GA^{low} phenotype. (A) Representative immunoblot of SGLT1 (~77 kDa) and membrane marker Na^+/K^+ ATPase-α subunit (~110 kDa) used as a loading control in total cell membrane lysates. (B) Quantification of SGLT1 protein expression. Data from three independent experiments (mean ± SEM); *p ≤ 0.05 and **p ≤ 0.01 (Student's two-tailed t-test). (C) Representative immunofluorescence confocal images (XY and XZ) of monolayers immunostained for SGLT1. Images are representative of three independent experiments. Scale bar, 10 μm. Note that differentiated cells are taller compared to undifferentiated cells in the enteroid monolayers. GA, glucose absorption; BMI, body mass index; UD, undifferentiated; DF, differentiated.

3.5. Elevated gluconeogenesis contributed significantly to the increase in basolateral glucose deposited by enteroid monolayers from the BMI^{obese}GA^{high} phenotypes

The expression of rate-limiting gluconeogenic enzymes phosphoenolpyruvate carboxykinase 1 (PEPCK1) and glucose-6-phosphatase (G6Pase) in human enterocytes indicates that the proximal small intestine might contribute to *de novo* glucose synthesis [39]. We found that PEPCK1 protein expression was significantly upregulated in the DF monolayers (~27-fold) and UD monolayers (~20-fold) from the BMI^{obese}GA^{high} group compared to the lean enteroid monolayers (Figure 5A,B). G6Pase mRNA levels were significantly increased (~26-fold) in the DF monolayers from the BMI^{obese}GA^{high} phenotype compared to the lean cultures (Figure 5C). The increased expression levels of gluconeogenic enzymes indicated that gluconeogenesis could also contribute to high blood glucose in obesity.

To test whether elevated gluconeogenic enzymes increase glucose production by enterocytes in obesity, we incubated DF monolayers from cultures of the BMI^{lean}GA^{low} and BMI^{obese}GA^{high} groups in glucose-free solutions containing gluconeogenic substrates and measured the amount of glucose deposited into the basolateral media. Apical exposure of the DF monolayers to 2 mM of pyruvate/20 mM of lactate significantly increased the basolateral glucose concentration in the BMI^{obese}GA^{high} monolayers but not in the lean enteroids, in which the basolateral glucose concentration was below detection levels (Figure 6A). These data indicated that *de novo* glucose synthesis via elevated expression of gluconeogenic enzymes is increased in obesity. Fructose feeding induces significant increases in the expression of intestinal fructolytic and gluconeogenic enzymes in mice [40], and ingested fructose is metabolized in the small intestine via gluconeogenesis [25,40]. We hypothesized that in the BMI^{obese}GA^{high} enteroids, fructose uptake via elevated apical GLUT5 followed by increased fructose metabolism via elevated gluconeogenic enzymes might significantly contribute to elevated glucose levels. We used apical fructose to assess the possible contribution of this dietary sugar to the basolateral glucose deposit via gluconeogenesis. Exposure to 70 mM of apical fructose for 3 h significantly increased the basolateral glucose concentration in the DF monolayers from BMI^{obese}GA^{high} phenotype but not in the lean phenotype (Figure 6A). These results indicated that in the BMI^{obese}GA^{high} group, increased GLUT5 expression led to increased fructose uptake, which served as a substrate for *de novo* glucose production.

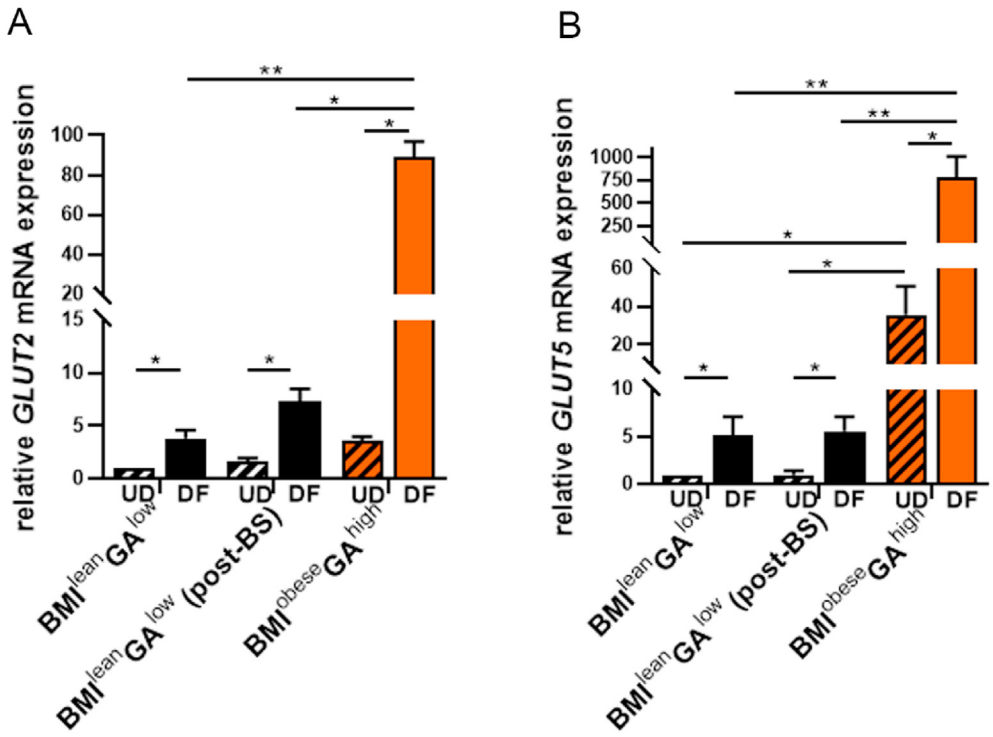

Figure 3: GLUT2 and GLUT5 mRNA expression levels were significantly upregulated in enteroid cultures derived from the $BMI^{obese}GA^{high}$ phenotype compared to the $BMI^{lean}GA^{low}$ phenotype. qPCR analysis of GLUT2 mRNA (A) and GLUT5 mRNA (B) expression in the UD and DF enteroid cultures. Data are normalized to 18S mRNA expression. Data from three independent experiments (mean ± SEM); *$p \leq 0.05$, **$p \leq 0.01$, and ***$p \leq 0.001$ (Student's two-tailed t-test). GA, glucose absorption; BMI, body mass index; UD, undifferentiated; DF, differentiated.

To examine the contribution of GLUT5 and GLUT2 to fructose uptake, we conducted pharmacological inhibition studies using MSNBA (a GLUT5 inhibitor) [41] and phloretin (a GLUT2 inhibitor). The DF monolayers from the $BMI^{obese}GA^{high}$ phenotype were treated apically for 3 h with 70 mM of fructose in the presence of 500 μM of MSNBA or 400 μM of PT. Inhibition of either GLUT2 or GLUT5 significantly decreased the basolateral glucose concentration (Figure 6B), indicating that both GLUT2 and GLUT5 are involved in luminal fructose uptake, and their inhibition decreases basolateral glucose deposition.

We next measured the contribution of gluconeogenesis to the basolateral glucose concentration in the DF monolayers from the $BMI^{lean}GA^{low}$ and $BMI^{obese}GA^{high}$ phenotypes (Figure 6C) treated with 70 mM of fructose for 16 h. The DF monolayers from the $BMI^{obese}GA^{high}$ phenotype had significantly higher basolateral glucose concentrations compared to the $BMI^{lean}GA^{low}$ phenotype. Collectively these data suggested that increased basolateral glucose deposition by gluconeogenesis can also substantially contribute to obesity.

4. DISCUSSION

We used human stem cell-derived enteroids as an *ex vivo* model of the small intestinal epithelium [27,28,30,31] to mimic the abnormal absorption and metabolism of dietary sugars associated with obesity. Using enteroids derived from 19 patients with a wide spectrum of BMIs, we showed four different glucose-absorption phenotypes. We were able to identify two different physiologic traits in morbidly obese patients: low or high epithelial sugar absorption. Enteroids from patients representing the $BMI^{obese}GA^{high}$ phenotype supported previous findings that showed increased expression of carbohydrate transporters and increased glucose absorption in obesity [10,23,42–45]. This phenotype is also characterized by a significant elevation in intestinal epithelial gluconeogenesis, a novel observation. Our findings suggested that at equal concentrations of dietary glucose, patients with the $BMI^{obese}GA^{high}$ phenotype might transport more glucose into the systemic circulation than non-obese patients. In future studies, it will be important to test the contribution of intestinal carbohydrate transport and metabolic abnormalities to glucose levels in the systemic circulation and evaluate the importance of their role in obesity and metabolic diseases in this category of patients. These data also provide a possible mechanistic explanation for the inability of changes in diet to combat morbid obesity [2–4]. However, our enteroid studies showed that this occurs only in a subset of obese patients. We found another morbidly obese phenotype with low glucose absorption ($BMI^{obese}GA^{low}$), and these findings match the presence of normoglycemic and hyperglycemic morbidly obese subjects [46]. The uptake and metabolism of amino acids and lipids are altered in obesity, suggesting that pathways other than carbohydrate uptake and metabolism may play a significant role in $BMI^{obese}GA^{low}$ phenotype patients. Our enteroid data on differential glucose absorption in morbidly obese individuals strongly supports a recent continuous glucose-monitoring study that identified several "glucotypes" based on the variability in blood glucose levels [47].

We demonstrated that all of the enteroids from the lean group (including post-BS cases) exhibited low glucose absorption and lacked gluconeogenic activity, similar to that measured in the lean BS naïve subjects. Our data matched results obtained by comparing human small intestinal samples pre- and post-BS in which SGLT1 and GLUT2 protein expression was increased in $BMI^{obese}GA^{high}$ obese patients

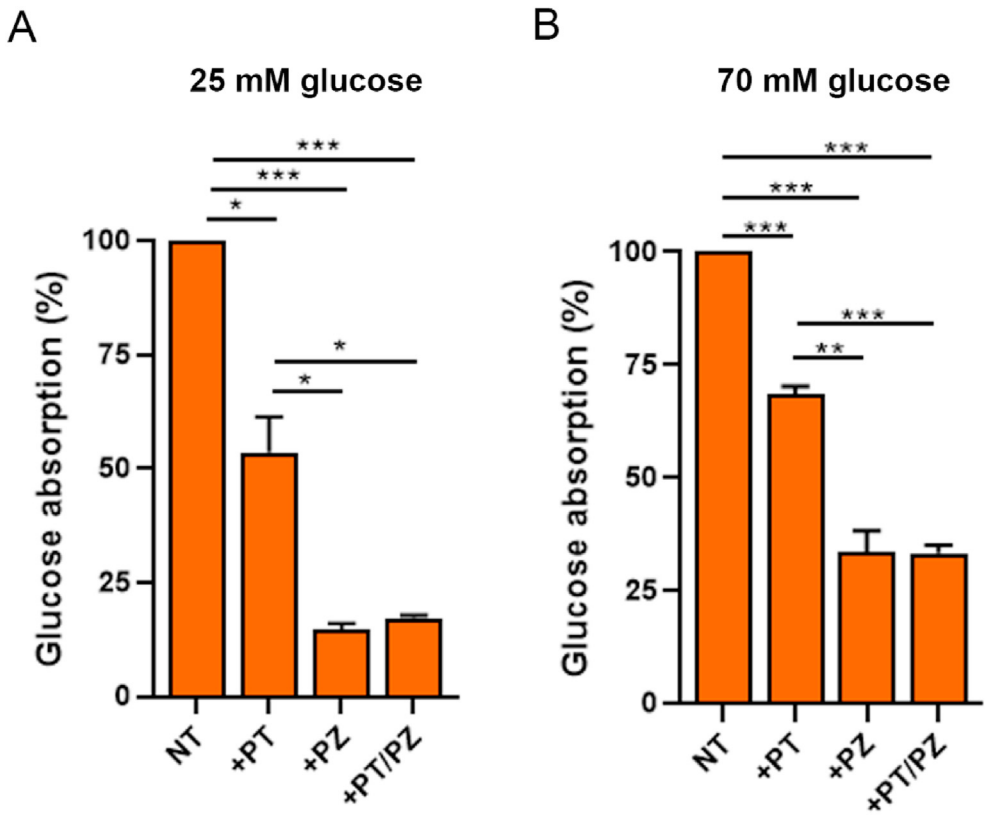

Figure 4: Inhibition of either SGLT1 or GLUT2 significantly decreased glucose absorption in differentiated enteroid cultures derived from the $BMI^{obese}GA^{high}$ phenotype. Effects of 50 μM of phloridzin (PZ, an SGLT1 inhibitor), 50 μM of phloretin (PT, a GLUT2 inhibitor), or their combination on glucose absorption in DF monolayers derived from the $BMI^{obese}GA^{high}$ phenotype at 120 min of exposure to either 25 mM (A) or 70 mM (B) of apical glucose. The basolateral glucose concentration in each experiment was normalized to the value of the NT (not treated) sample, which was set at 100%. Data from three independent experiments (mean ± SEM). Each experiment was conducted in triplicate; *p ≤ 0.05, **p ≤ 0.01, and ***p ≤ 0.001 (Student's two-tailed t-test). NT, not treated; GA, glucose absorption; BMI, body mass index; UD, undifferentiated; DF, differentiated.

compared to lean subjects, while the expression level of these proteins in post-BS was similar to lean controls [48]. Our studies are the first to measure transepithelial glucose absorption in $BMI^{obese}GA^{high}$ enteroids and emphasize the potential significance of the intestinal contribution to blood glucose levels in obesity. Inhibition of either SGLT1 or GLUT2 significantly decreased glucose absorption, indicating that these transporters might be potential targets for hyperglycemia in the $BMI^{obese}GA^{high}$ subset of obese patients. Recent clinical studies using

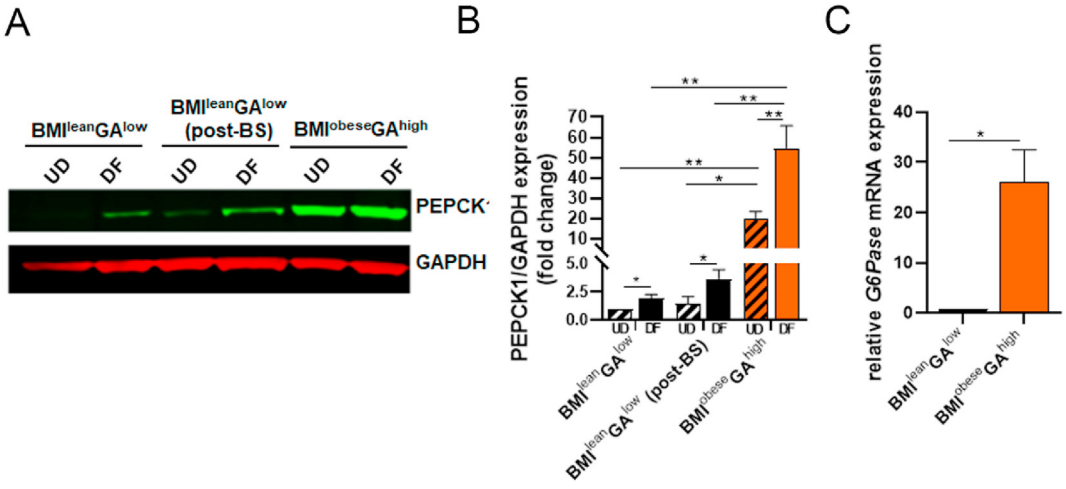

Figure 5: Gluconeogenic enzymes were significantly upregulated in enteroid cultures derived from the $BMI^{obese}GA^{high}$ phenotype compared to the $BMI^{lean}GA^{low}$ phenotype. (A) Representative immunoblot of PEPCK1 (~69 kDa) and housekeeping marker GAPDH (~36 kDa) in total cell lysates. (B) Quantification of PEPCK1 protein expression. (C) qPCR analysis of glucose-6-phosphatase (G6Pase) mRNA levels in differentiated enteroid cultures derived from the $BMI^{obese}GA^{high}$ phenotype and $BMI^{lean}GA^{low}$ phenotype subjects. Data are normalized to 18S mRNA expression. Data from three independent experiments (mean ± SEM); *p ≤ 0.05 and **p ≤ 0.01 (Student's two-tailed t-test). GA, glucose absorption; BMI, body mass index; UD, undifferentiated; DF, differentiated.

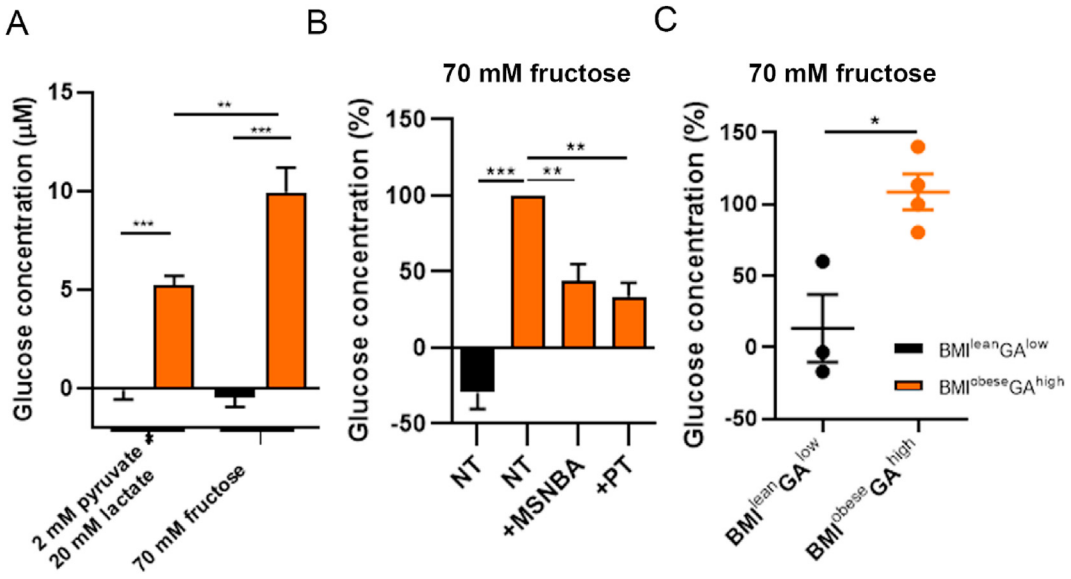

Figure 6: Enteroid monolayers representing the $BMI^{obese}GA^{high}$ demonstrated significantly elevated gluconeogenesis with dietary fructose as a potential substrate. (A) Basolateral glucose concentration after apical treatment of the DF monolayers from the $BMI^{obese}GA^{high}$ phenotype or $BMI^{lean}GA^{low}$ phenotype with either 2 mM of pyruvate/20 mM of lactate or 70 mM of fructose for 3 h. Basolateral glucose concentration in enteroid monolayers representing the $BMI^{lean}GA^{low}$ phenotype was below the detection limit. (B) Effects of 500 μM of -[4-(methylsulfonyl)-2-nitrophenyl]-1,3-benzodioxol-5-amine (MSNBA, a GLUT5 inhibitor) or 400 μM of phloretin (PT, a GLUT2 inhibitor) on the basolateral glucose concentration in the DF monolayers derived from the $BMI^{obese}GA^{high}$ phenotype at 3 h of exposure to 70 mM of apical fructose. Basolateral glucose concentration in each experiment was normalized to the value of the NT (not treated) enteroid culture #9 of the $BMI^{obese}GA^{high}$ group, which was set at 100%. Basolateral glucose concentration in monolayers representing the $BMI^{lean}GA^{low}$ phenotype (black bar) was below the detection limit. (C) The basolateral glucose concentration after apical treatment of the DF monolayers from the $BMI^{obese}GA^{high}$ phenotype ($n = 3$ subjects) or $BMI^{lean}GA^{low}$ phenotype ($n = 4$ subjects) with 70 mM of fructose for 16 h. Data in each experiment were normalized to the value of enteroid culture #9, which was set at 100%. (A–C) Data from three independent experiments (mean ± SEM); each experiment was conducted in triplicate; *$p \leq 0.05$, **$p \leq 0.01$, and ***$p \leq 0.001$ (Student's two-tailed t-test). NT, not treated; GA, glucose absorption; BMI, body mass index; UD, undifferentiated; DF, differentiated.

licogliflozin, a dual SGLT1/2 inhibitor, showed promising results in decreasing blood glucose and body weight of obese patients [49].

Interestingly, we observed significant differences in glucose absorption between enteroids from the BS naïve lean subjects and those from the post-BS patients, despite the lack of significant differences in the expression levels of sugar transporters between these two groups. Additional consideration for differences in signaling, intracellular localization, and subcellular trafficking could contribute to different glucose-absorption profiles [23,59]. Dynamic regulation of glucose transport by protein trafficking has been reported for GLUT4 [60]. Therefore, possible mechanisms that could explain the differences in glucose absorption between these enteroid groups at high luminal glucose concentrations that should be addressed in future studies include: a) differences in the localization of GLUT2 levels under basal conditions, b) differences in glucose-dependent GLUT2 trafficking to the apical plasma membrane to facilitate the uptake of excess glucose, and c) differences in post-transcriptional and post-translational regulation of SGLT1 and/or GLUT2.

In addition, our functional data in human enteroids demonstrated that intestinal epithelial gluconeogenesis may significantly contribute to elevated blood glucose in obesity. Fructose is the main gluconeogenic substrate transported into enterocytes by GLUT5, the apical fructose transporter that is elevated in the intestine of T2D patients [20]. Our data showed for the first time the functional link between GLUT5 and the upregulation of the major rate-limiting gluconeogenic enzymes PEPCK1 and G6Pase, which resulted in a significant increase in glucose deposited into the serosa following dietary fructose uptake. Pharmacologic inhibition of GLUT5 decreased glucose production via gluconeogenesis, suggesting that GLUT5 may also be a valuable target in treating obesity. The contribution of gluconeogenesis to high serum glucose levels in obese and T2D patients is essentially unknown. Portal vein glucose measurements cannot separate the contribution of intestinal glucose absorption and gluconeogenesis; therefore, a relevant *in vitro* model of the human intestinal epithelium is required to discriminate how each contributes to high blood glucose. Although data from an animal model of T2D suggested that gluconeogenesis might increase in the gut epithelium post-BS surgery [50], these findings are not supported by human clinical data. In contrast, direct simultaneous measurement of fasting glucose in portal and central venous blood before and 6 days after RYGB provide no evidence to support the hypothesis that intestinal gluconeogenesis contributes to the resolution of T2DM after RYGB [51]. In agreement with our data, higher PEPCK1 expression and higher enzymatic activity of G6Pase was detected in the jejunum of morbidly obese patients with high insulin resistance [52]. Similarly, decreased relative abundance of PEPCK1 and G6Pase was observed in all segments of the intestine after RYGB [53]. Taken together, these data indicate that intestinal gluconeogenesis might contribute to high blood glucose in obesity in humans and successful BS surgery might be accompanied by a decrease in the portion of blood glucose derived from intestinal gluconeogenesis.

Collectively, our data demonstrate that intestinal glucose absorption via transport and gluconeogenesis might contribute to high blood glucose levels in a subset of morbidly obese patients (Figure 7). Based on these data, we suggest that the decrease in serum glucose concentrations that occurs after BS [8,9] might be partially due to the minimization of the intestinal contribution to overall blood glucose levels. It remains to be determined whether successful BS could be predicted by high intestinal glucose absorption and/or gluconeogenesis prior to surgery. However, targeting the molecular steps involved in intestinal glucose

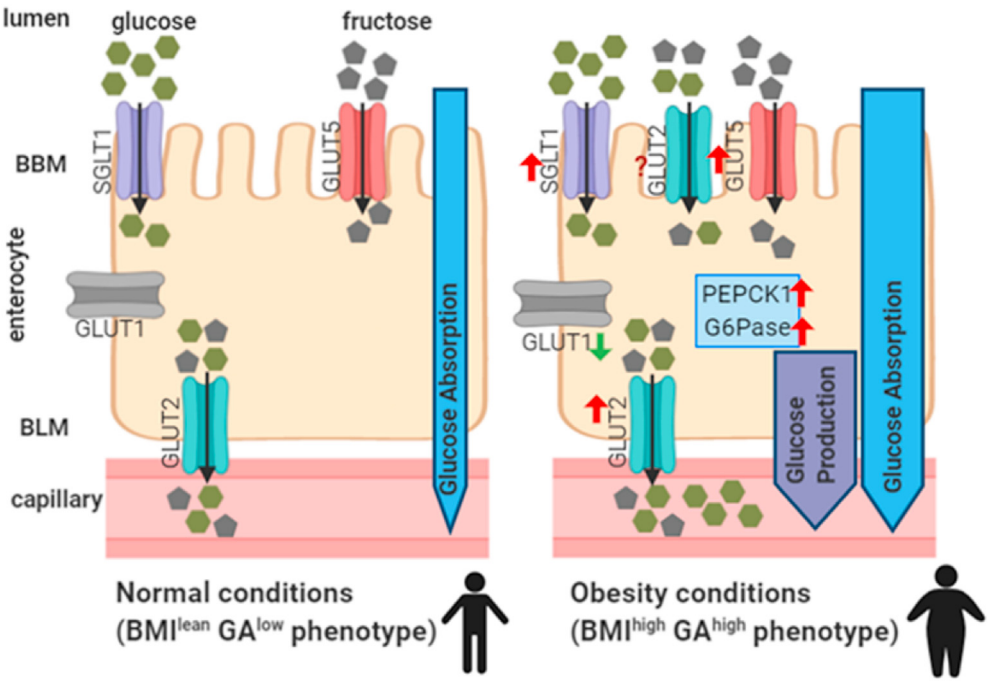

Figure 7: Schematic diagram of glucose transporters, glucose absorption, and gluconeogenesis in enterocytes under normal and obesity conditions. Under normal conditions, SGLT1 and GLUT5 [16] are localized to the apical membrane of enterocytes transporting glucose and fructose respectively into the cells. GLUT2 is localized at the basolateral membrane and transports glucose and fructose out of the cells into the bloodstream [13,14]. GLUT1 has lateral and intracellular localization. In obesity conditions, expression levels of SGLT1 and GLUT2 increase, resulting in increased glucose absorption. GLUT1 levels decrease. Additionally, GLUT5 levels and gluconeogenesis enzymes (PEPCK1 and G6Pase) increase, resulting in increased production of glucose in enterocytes that are transported to the bloodstream. GLUT2 might be localized apically [23,24]. The schematic was created using biorender.com.

transport and gluconeogenesis may represent a pathway for the development of novel drugs to treat metabolic diseases. These data also suggest that multiple molecular targets must be considered when using therapeutic approaches to duplicate the effects of BS on the instant decrease in blood glucose levels.

Our data confirmed observations [6] that the "non-intestinal" GLUT1 glucose transporter is expressed in human enterocytes. Immunofluorescence demonstrated that GLUT1 was mainly localized to the lateral membrane and intracellularly in the UD monolayers and intracellularly in the DF monolayers from the $BMI^{lean}GA^{low}$ group (Supplementary Fig. 5C). Interestingly, both GLUT1 expression levels and intracellular distribution were greatly diminished in the $BMI^{obese}GA^{high}$ enteroids (Supplementary Fig. 5A-C). Differentiation decreased GLUT1 protein levels and increased its intracellular presence, indicating potential trafficking to the cytosol. Thioredoxin-interacting protein (TXNIP) is involved in GLUT1 endocytosis and degradation [54]. We observed an increase in TXNIP levels upon differentiation in enteroids (data not shown), suggesting a potential explanation for the decrease in GLUT1. GLUT1 was not associated with glucose absorption (Supplementary Fig. 5D), suggesting that GLUT1 might supply glucose to proliferating stem cells in undifferentiated enteroids, which require energy but express low levels of other sugar transporters and gluconeogenic enzymes. The role of GLUT1 in the intestinal epithelium remains to be examined.

Human small intestinal enteroid cultures obtained from different patients can retain the donor phenotype [55]. These data support our findings that human enteroid cultures preserve the phenotypic differences between epithelia from obese, overweight, lean, and post-BS subjects for multiple passages. Our findings demonstrated for the first time that stable long-term changes in gene regulation in intestinal stem cells occur in obesity. Enteroids retain these patient characteristics and could serve as a model to study cellular and molecular changes associated with obesity. This conclusion was supported by recent observations that disease phenotypes of several chronic intestinal disorders such as celiac disease [56,57] or inflammatory bowel disease [35,58] are preserved in human intestinal enteroids. This allows for relevant *in vitro* studies using human enteroids to investigate disease phenotypes, mechanisms of disease progression, and individual therapeutic options.

A limitation of our study is the small number of subjects per group and the lack of detailed clinical information regarding the subjects; therefore, conclusions regarding the clinical relevance of this study cannot be generalized. However, our study demonstrated the presence of phenotypic differences between enteroid cultures that were conserved *ex vivo* for at least 15 passages and provided evidence that patient-derived enteroids can be used in more detailed studies to understand the pathophysiology of obesity in a model that retains the patient-specific disease phenotype. Future studies are needed to delineate the contribution of clinical factors to the observed glucose absorption/gluconeogenesis phenotypes. It is also necessary to address the direct role of bariatric surgery in the possible changes in intestinal carbohydrate transport and metabolism by analysis of glucose absorption/gluconeogenesis in collections of pre- and post-BS tissue/enteroids from the same subjects and evaluate enteroids with clinical data of patients at the time of tissue collection.

We conclude that obesity is characterized by significant and stable changes in the expression and activity of major dietary sugar transporters and gluconeogenic enzymes in human intestinal epithelium in a subset of morbidly obese patients. These changes lead to significant increases in glucose absorption that might substantially contribute to

high blood glucose levels in obesity. Human enteroid monolayers that preserve the patient phenotype in long-term cultures represent a reliable and robust model to study the consequences of obesity and search for effective therapeutic interventions.

AUTHOR CONTRIBUTIONS

N.M.H., J.Y., K.F.J., and N.W.B. conducted the experiments. N.M.H., N.C.Z., and O.K. designed the experiments. N.M.H., N.C.Z., and O.K. analyzed the results. V.S. and V.K. acquired the patient specimens. N.M.H. and O.K. prepared the manuscript. N.M.H., S.E.B., M.K.E., V.K., N.C.Z., and O.K. discussed the results and edited the manuscript. The final manuscript was approved by all of the authors.

FUNDING

This study was funded by NIH grants P01 AI125181 and P30 DK089502.

ACKNOWLEDGMENTS

We acknowledge the Integrated Physiology, Imaging, and Translational Research Enhancement Cores of the Hopkins Conte Digestive Disease Basic and Translational Research Core Center. The authors thank Dr. James Potter, Dr. Steven Brant (Hopkins), and Xi-Lei Zeng (Baylor) for their assistance in acquiring patient specimens from which proximal small intestinal enteroid lines were established. We thank Dr. Mark Donowitz for his helpful suggestions and critical reading of the manuscript. The manuscript is available as a preprint (https://doi.org/10.1101/2020.05.29.123737).

CONFLICT OF INTEREST

None declared.

APPENDIX A. SUPPLEMENTARY DATA

Supplementary data to this article can be found online at https://doi.org/10.1016/j.molmet.2020.101129.

REFERENCES

[1] Kitahara, C.M., Flint, A.J., Berrington de Gonzalez, A., Bernstein, L., Brotzman, M., MacInnis, R.J., et al., 2014. Association between class III obesity (BMI of 40-59 kg/m2) and mortality: a pooled analysis of 20 prospective studies. PLoS Medicine 11(7):e1001673.

[2] Gudzune, K.A., Doshi, R.S., Mehta, A.K., Chaudhry, Z.W., Jacobs, D.K., Vakil, R.M., et al., 2015. Efficacy of commercial weight-loss programs: an updated systematic review. Annals of Internal Medicine 162(7):501–512.

[3] Sethi, M., Parikh, M., 2015. Bariatric surgery versus intensive medical weight management for type 2 diabetes. Advances in Surgery 49:157–171.

[4] Swift, D.L., Johannsen, N.M., Lavie, C.J., Earnest, C.P., Church, T.S., 2014. The role of exercise and physical activity in weight loss and maintenance. Progress in Cardiovascular Diseases 56(4):441–447.

[5] Bradley, D., Magkos, F., Klein, S., 2012. Effects of bariatric surgery on glucose homeostasis and type 2 diabetes. Gastroenterology 143(4):897–912.

[6] Cavin, J.B., Couvelard, A., Lebtahi, R., Ducroc, R., Arapis, K., Voitellier, E., et al., 2016. Differences in alimentary glucose absorption and intestinal disposal of blood glucose after roux-en-Y gastric bypass vs sleeve gastrectomy. Gastroenterology 150(2):454–464 e459.

[7] Odstrcil, E.A., Martinez, J.G., Santa Ana, C.A., Xue, B., Schneider, R.E., Steffer, K.J., et al., 2010. The contribution of malabsorption to the reduction in net energy absorption after long-limb Roux-en-Y gastric bypass. American Journal of Clinical Nutrition 92(4):704–713.

[8] Roslin, M.S., Dudiy, Y., Weiskopf, J., Damani, T., Shah, P., 2012. Comparison between RYGB, DS, and VSG effect on glucose homeostasis. Obesity Surgery 22(8):1281–1286.

[9] Vidal, J., Jimenez, A., de Hollanda, A., Flores, L., Lacy, A., 2015. Metabolic surgery in type 2 diabetes: roux-en-Y gastric bypass or sleeve gastrectomy as procedure of choice? Current Atherosclerosis Reports 17(10):58.

[10] Nguyen, N.Q., Debreceni, T.L., Bambrick, J.E., Chia, B., Wishart, J., Deane, A.M., et al., 2015. Accelerated intestinal glucose absorption in morbidly obese humans: relationship to glucose transporters, incretin hormones, and glycemia. The Journal of Cinical Endocrinology and Metabolism 100(3):968–976.

[11] Gorboulev, V., Schurmann, A., Vallon, V., Kipp, H., Jaschke, A., Klessen, D., et al., 2012. Na(+)-D-glucose cotransporter SGLT1 is pivotal for intestinal glucose absorption and glucose-dependent incretin secretion. Diabetes 61(1):187–196.

[12] Wright, E.M., Loo, D.D., Hirayama, B.A., 2011. Biology of human sodium glucose transporters. Physiological Reviews 91(2):733–794.

[13] Cheeseman, C.I., 1993. GLUT2 is the transporter for fructose across the rat intestinal basolateral membrane. Gastroenterology 105(4):1050–1056.

[14] Thorens, B., Cheng, Z.Q., Brown, D., Lodish, H.F., 1990. Liver glucose transporter: a basolateral protein in hepatocytes and intestine and kidney cells. American Journal of Physiology 259(6 Pt 1):C279–C285.

[15] Kellett, G.L., Helliwell, P.A., 2000. The diffusive component of intestinal glucose absorption is mediated by the glucose-induced recruitment of GLUT2 to the brush-border membrane. Biochemical Journal 350(Pt 1):155–162.

[16] Davidson, N.O., Hausman, A.M., Ifkovits, C.A., Buse, J.B., Gould, G.W., Burant, C.F., et al., 1992. Human intestinal glucose transporter expression and localization of GLUT5. American Journal of Physiology 262(3 Pt 1):C795–C800.

[17] Barone, S., Fussell, S.L., Singh, A.K., Lucas, F., Xu, J., Kim, C., et al., 2009. Slc2a5 (Glut5) is essential for the absorption of fructose in the intestine and generation of fructose-induced hypertension. Journal of Biological Chemistry 284(8):5056–5066.

[18] Boyer, S., Sharp, P.A., Debnam, E.S., Baldwin, S.A., Srai, S.K., 1996. Streptozotocin diabetes and the expression of GLUT1 at the brush border and basolateral membranes of intestinal enterocytes. FEBS Letters 396(2–3):218–222.

[19] Burant, C.F., Flink, S., DePaoli, A.M., Chen, J., Lee, W.S., Hediger, M.A., et al., 1994. Small intestine hexose transport in experimental diabetes. Increased transporter mRNA and protein expression in enterocytes. Journal of Clinical Investigation 93(2):578–585.

[20] Dyer, J., Wood, I.S., Palejwala, A., Ellis, A., Shirazi-Beechey, S.P., 2002. Expression of monosaccharide transporters in intestine of diabetic humans. American Journal of Physiology - Gastrointestinal and Liver Physiology 282(2):G241–G248.

[21] Miyamoto, K., Hase, K., Takagi, T., Fujii, T., Taketani, Y., Minami, H., et al., 1993. Differential responses of intestinal glucose transporter mRNA transcripts to levels of dietary sugars. Biochemical Journal 295(Pt 1):211–215.

[22] Miyauchi, E., Tachikawa, M., Decleves, X., Uchida, Y., Bouillot, J.L., Poitou, C., et al., 2016. Quantitative atlas of cytochrome P450, UDP-glucuronosyltransferase, and transporter proteins in jejunum of morbidly obese subjects. Molecular Pharmaceutics 13(8):2631–2640.

[23] Ait-Omar, A., Monteiro-Sepulveda, M., Poitou, C., Le Gall, M., Cotillard, A., Gilet, J., et al., 2011. GLUT2 accumulation in enterocyte apical and intracellular membranes: a study in morbidly obese human subjects and ob/ob and high fat-fed mice. Diabetes 60(10):2598–2607.

[24] Monteiro-Sepulveda, M., Touch, S., Mendes-Sa, C., Andre, S., Poitou, C., Allatif, O., et al., 2015. Jejunal T cell inflammation in human obesity correlates with decreased enterocyte insulin signaling. Cell Metabolism 22(1):113–124.

[25] Jang, C., Hui, S., Lu, W., Cowan, A.J., Morscher, R.J., Lee, G., et al., 2018. The small intestine converts dietary fructose into glucose and organic acids. Cell Metabolism 27(2):351—361 e353.
[26] Soty, M., Gautier-Stein, A., Rajas, F., Mithieux, G., 2017. Gut-brain glucose signaling in energy homeostasis. Cell Metabolism 25(6):1231—1242.
[27] Foulke-Abel, J., In, J., Yin, J., Zachos, N.C., Kovbasnjuk, O., Estes, M.K., et al., 2016. Human enteroids as a model of upper small intestinal ion transport Physiology and pathophysiology. Gastroenterology 150(3):638—649 e638.
[28] In, J., Foulke-Abel, J., Zachos, N.C., Hansen, A.M., Kaper, J.B., Bernstein, H.D., et al., 2016. Enterohemorrhagic Escherichia coli reduce mucus and intermicrovillar bridges in human stem cell-derived colonoids. Cell Mol Gastroenterol Hepatol 2(1):48—62 e43.
[29] In, J.G., Foulke-Abel, J., Clarke, E., Kovbasnjuk, O., 2019. Human colonoid monolayers to study interactions between pathogens, commensals, and host intestinal epithelium. Journal of Visualized Experiments 146.
[30] Sato, T., Stange, D.E., Ferrante, M., Vries, R.G., Van Es, J.H., Van den Brink, S., et al., 2011. Long-term expansion of epithelial organoids from human colon, adenoma, adenocarcinoma, and Barrett's epithelium. Gastroenterology 141(5):1762—1772.
[31] Sato, T., Vries, R.G., Snippert, H.J., van de Wetering, M., Barker, N., Stange, D.E., et al., 2009. Single Lgr5 stem cells build crypt-villus structures in vitro without a mesenchymal niche. Nature 459(7244):262—265.
[32] Heijmans, J., van Lidth de Jeude, J.F., Koo, B.K., Rosekrans, S.L., Wielenga, M.C., van de Wetering, M., et al., 2013. ER stress causes rapid loss of intestinal epithelial stemness through activation of the unfolded protein response. Cell Reports 3(4):1128—1139.
[33] Vrhovac, I., Balen Eror, D., Klessen, D., Burger, C., Breljak, D., Kraus, O., et al., 2015. Localizations of Na(+)-D-glucose cotransporters SGLT1 and SGLT2 in human kidney and of SGLT1 in human small intestine, liver, lung, and heart. Pflügers Archiv 467(9):1881—1898.
[34] Sjoqvist, A., Beeuwkes 3rd, R., 1990. Villus and crypt electrolyte and fluid transport during intestinal secretion. Acta Physiologica Scandinavica 139(1):203—210.
[35] Dotti, I., Mora-Buch, R., Ferrer-Picon, E., Planell, N., Jung, P., Masamunt, M.C., et al., 2017. Alterations in the epithelial stem cell compartment could contribute to permanent changes in the mucosa of patients with ulcerative colitis. Gut 66(12):2069—2079.
[36] Middendorp, S., Schneeberger, K., Wiegerinck, C.L., Mokry, M., Akkerman, R.D., van Wijngaarden, S., et al., 2014. Adult stem cells in the small intestine are intrinsically programmed with their location-specific function. Stem Cells 32(5):1083—1091.
[37] Zheng, Y., Scow, J.S., Duenes, J.A., Sarr, M.G., 2012. Mechanisms of glucose uptake in intestinal cell lines: role of GLUT2. Surgery 151(1):13—25.
[38] Zietek, T., Rath, E., Haller, D., Daniel, H., 2015. Intestinal organoids for assessing nutrient transport, sensing and incretin secretion. Scientific Reports 5:16831.
[39] Yanez, A.J., Nualart, F., Droppelmann, C., Bertinat, R., Brito, M., Concha II, , et al., 2003. Broad expression of fructose-1,6-bisphosphatase and phosphoenolpyruvate carboxykinase provide evidence for gluconeogenesis in human tissues other than liver and kidney. Journal of Cellular Physiology 197(2):189—197.
[40] Patel, C., Douard, V., Yu, S., Tharabenjasin, P., Gao, N., Ferraris, R.P., 2015. Fructose-induced increases in expression of intestinal fructolytic and gluconeogenic genes are regulated by GLUT5 and KHK. American Journal of Physiology - Regulatory, Integrative and Comparative Physiology 309(5):R499—R509.
[41] George Thompson, A.M., Ursu, O., Babkin, P., Iancu, C.V., Whang, A., Oprea, T.I., et al., 2016. Discovery of a specific inhibitor of human GLUT5 by virtual screening and in vitro transport evaluation. Scientific Reports 6:24240.
[42] Cui, X.L., Jiang, L., Ferraris, R.P., 2003. Regulation of rat intestinal GLUT2 mRNA abundance by luminal and systemic factors. Biochimica et Biophysica Acta 1612(2):178—185.
[43] Ferraris, R.P., 2001. Dietary and developmental regulation of intestinal sugar transport. Biochemical Journal 360(Pt 2):265—276.
[44] Herman, M.A., Samuel, V.T., 2016. The sweet path to metabolic demise: fructose and lipid synthesis. Trends in Endocrinology and Metabolism 27(10): 719—730.
[45] Kellett, G.L., Brot-Laroche, E., Mace, O.J., Leturque, A., 2008. Sugar absorption in the intestine: the role of GLUT2. Annual Review of Nutrition 28:35—54.
[46] Manders, R.J., Pennings, B., Beckers, C.P., Aipassa, T.I., van Loon, L.J., 2009. Prevalence of daily hyperglycemia in obese type 2 diabetic men compared with that in lean and obese normoglycemic men: effect of consumption of a sucrose-containing beverage. American Journal of Clinical Nutrition 90(3): 511—518.
[47] Hall, H., Perelman, D., Breschi, A., Limcaoco, P., Kellogg, R., McLaughlin, T., et al., 2018. Glucotypes reveal new patterns of glucose dysregulation. PLoS Biology 16(7):e2005143.
[48] Wolnerhanssen, B.K., Moran, A.W., Burdyga, G., Meyer-Gerspach, A.C., Peterli, R., Manz, M., et al., 2017. Deregulation of transcription factors controlling intestinal epithelial cell differentiation; a predisposing factor for reduced enteroendocrine cell number in morbidly obese individuals. Scientific Reports 7(1):8174.
[49] He, Y.L., Haynes, W., Meyers, C.D., Amer, A., Zhang, Y., Mahling, P., et al., 2019. The effects of licogliflozin, a dual SGLT1/2 inhibitor, on body weight in obese patients with or without diabetes. Diabetes, Obesity and Metabolism 21(6):1311—1321.
[50] Yan, Y., Zhou, Z., Kong, F., Feng, S., Li, X., Sha, Y., et al., 2016. Roux-en-Y gastric bypass surgery suppresses hepatic gluconeogenesis and increases intestinal gluconeogenesis in a T2DM rat model. Obesity Surgery 26(11):2683—2690.
[51] Hayes, M.T., Foo, J., Besic, V., Tychinskaya, Y., Stubbs, R.S., 2011. Is intestinal gluconeogenesis a key factor in the early changes in glucose homeostasis following gastric bypass? Obesity Surgery 21(6):759—762.
[52] Gutierrez-Repiso, C., Ho-Plagaro, A., Santiago-Fernandez, C., Garcia-Serrano, S., Rodriguez-Pacheco, F., Valdes, S., et al., 2020. Jejunal insulin signalling is increased in morbidly obese subjects with high insulin resistance and is regulated by insulin and leptin. Journal of Clinical Medicine 9(1).
[53] Wolff, B.S., Meirelles, K., Meng, Q., Pan, M., Cooney, R.N., 2009. Roux-en-Y gastric bypass alters small intestine glutamine transport in the obese Zucker rat. American Journal of Physiology - Gastrointestinal and Liver Physiology 297(3):G594—G601.
[54] Wu, N., Zheng, B., Shaywitz, A., Dagon, Y., Tower, C., Bellinger, G., et al., 2013. AMPK-dependent degradation of TXNIP upon energy stress leads to enhanced glucose uptake via GLUT1. Molecular Cell 49(6):1167—1175.
[55] Saxena, K., Simon, L.M., Zeng, X.L., Blutt, S.E., Crawford, S.E., Sastri, N.P., et al., 2017. A paradox of transcriptional and functional innate interferon responses of human intestinal enteroids to enteric virus infection. Proceedings of the National Academy of Sciences of the U S A 114(4):E570—E579.
[56] Freire, R., Ingano, L., Serena, G., Cetinbas, M., Anselmo, A., Sapone, A., et al., 2019. Human gut derived-organoids provide model to study gluten response and effects of microbiota-derived molecules in celiac disease. Scientific Reports 9(1):7029.
[57] Pietz, G., De, R., Hedberg, M., Sjoberg, V., Sandstrom, O., Hernell, O., et al., 2017. Immunopathology of childhood celiac disease-Key role of intestinal epithelial cells. PloS One 12(9):e0185025.
[58] Angus, H.C.K., Butt, A.G., Schultz, M., Kemp, R.A., 2019. Intestinal organoids as a tool for inflammatory bowel disease Research. Frontiers of Medicine 6:334.
[59] Koepsell, H., 2020. Glucose transporters in the small intestine in health and disease. Pflügers Archiv 472(9):1207—1248.
[60] Klip, A., McGraw, T.E., James, D.E., 2019. Thirty sweet years of GLUT4. Journal of Biological Chemistry 294(30):11369—11381.

